SEISMIC JACKETING OF RC COLUMNS FOR ENHANCED AXIAL LOAD CARRYING PERFORMANCE

Keh-Chyuan Tsai* and Min-Lang Lin
Department of Civil Engineering
National Taiwan University
Taipei, Taiwan 106, R.O.C.

Key Words: steel jacketing, CFRP jacketing, octagon shape.

ABSTRACT

Axial compression test results for square RC columns incorporating Taiwanese construction practice in the placement of stirrups and various kinds of jacketing schemes are presented. The jacketing schemes include circular, octagonal and square shapes. The jacketing materials vary from steel plate to carbon fiber reinforced polymer (CFRP) composites. It is found from the monotonic axial load test results that the failure mode of the benchmark non-retrofitted specimen is identical to that observed in real damage cases subsequent to the 1999 Chi-Chi Taiwan earthquake. The benchmark specimen developed its design strength but a non-ductile failure mode occurred soon after the peak load was reached. Among the retrofitted specimens, the steel jacketed specimens exhibit not only greatly enhanced load carry capacity but also excellent ductility performance. Test results show that CFRP sheets are effective in increasing the column axial strength, but the sheets could fracture suddenly in high strain conditions due to their brittle material characteristics. Test results indicate that CFRP sheet wrapping in general is not as effective as steel jacketing in improving the axial ductility capacity of RC columns. However, the proposed octagon-shaped CFRP wrapping scheme exhibits an improved performance compared to rectangular-wrapped columns using the same layers of CFRP sheets. Tests confirm that all octagonal steel or CFRP jacketed specimens have axial loading capacities more than 2 times the nominal capacity.

I. INTRODUCTION

Lessons learned from the 1999 Chi-Chi Taiwan earthquake indicate that inadequate axial load carrying and axial ductility capacities of the columns, among many other problems, are key factors responsible for the collapse of many reinforced concrete buildings. As shown in Fig. 1, commonly encountered are columns with splices with inadequate development length or located in the hinge region, or stirrups with 90 degree hooks, or widely spaced stirrups resulting in unconfined plastic hinge zones. Strong-beam weak-columns systems were apparently common, which might have resulted in numerous story collapses, following excessive column compressive load, induced by large overturning moments. In order to gain insights into the compression load carry characteristics and the effectiveness of various kinds

*Correspondence addressee

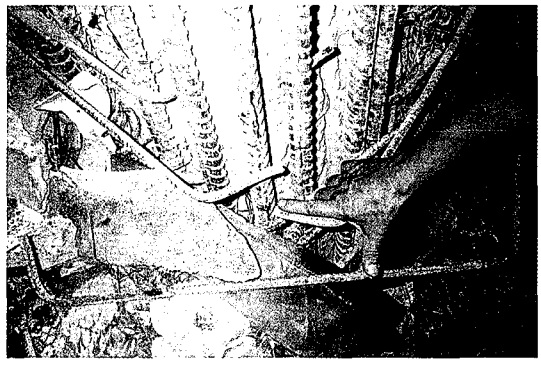

(a)

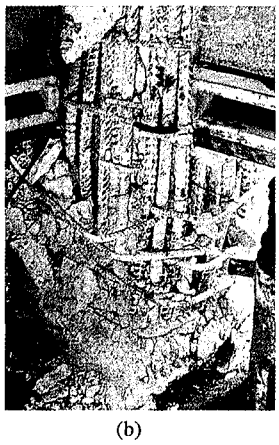

(b)

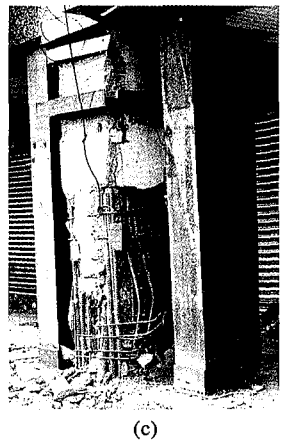

(c)

Fig. 1 Real damage cases subsequent to the 1999 Chi-Chi Earthquake

of seismic jacketing schemes on the aforementioned deficient rectangular reinforced concrete columns, an experimental test program was launched in the National Taiwan University (Tsai and Lin, 2002). In a recent study on the seismic retrofit of rectangular RC bridge columns (Tsai and Lin, 2001; Tsai *et al.*, 2000), the use of octagonal-shaped steel jacketing has been proposed and extensively tested for bridge columns subjected to a low axial compressive stress but very severe cyclic flexural or shear demands. These test results have confirmed that properly proportioned octagonal steel jackets can improve the cyclic strength and ductility performance of bridge columns deficient in flexural or shear strength. Research results also indicate that rectangular steel jacketing cannot effectively provide lateral confinement due to the bulging out of the jacket (Sun *et al.*, 1993; Harries *et al.*, 1999; Tsai and Lin, 2001). This study focuses on investigating the effectiveness of steel plate and carbon fiber reinforced plastic (CFRP) jacketing schemes in improving the axial strength and axial ductility performance of existing rectangular RC building columns subjected to high axial loads. A total of 12 square RC column specimens, using transverse reinforcing tie details commonly found in Taiwan were tested.

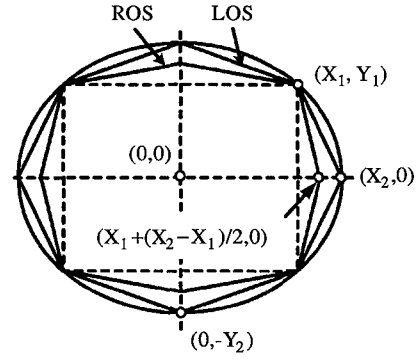

Fig. 2 Dimensions of octagonal jacketing schemes

The external jackets adopted in these specimens were configured in circular, square and octagonal shapes.

II. RETROFIT DESIGN

The design of octagonal steel jacketing is introduced herein. In the seismic retrofit of rectangular RC bridge columns, elliptical steel jacketing has been found effective (Sun *et al.*, 1993). The ellipse circumscribes the rectangle while the octagon can be conveniently defined based on the circumscribing ellipse and the original rectangle as shown in Fig. 2. The dimensions of the ellipse can be expressed as:

$$\frac{X^2}{X_2^2}+\frac{Y^2}{Y_2^2}=1 \tag{1}$$

where X_2 and Y_2 are the long and short axes of the ellipse, respectively, and assume:

$$X_2=KY_2 \tag{2}$$

Substituting Eq. (2) and (X_1, Y_1) into Eq. (1) yields:

$$Y_2=\sqrt{(\frac{X_1}{K})^2+Y_1^2} \tag{3}$$

Applying the rule of minimum elliptical area:

$$Min\, f\,(X_2, Y_2)=Min\, f\,(\pi X_2 Y_2) \tag{4}$$

substituting Eqs. (2) and (3) into Eq. (4), and taking variation yields:

$$K=\frac{X_1}{Y_1} \tag{5}$$

thus, X_2 and Y_2 can be expressed as:

$$X_2=\sqrt{2}X_1 \tag{6}$$

$$Y_2=\sqrt{2}Y_1 \tag{7}$$

The long and short axes of the ellipse can be determined using Eqs. (6) and (7), respectively. If the four corner points of the rectangle and the four intersecting points, of the ellipse, and the two axes, are connected, these eight points define an octagon (Fig. 2), denoted the "Large Octagonal Shape". Both the elliptical and the associated octagonal retrofit schemes will increase the column cross sectional substantially. Therefore, for a case when a more compact scheme is desired, the reduced octagon shape has been proposed. If the dimension of X_2 is reduced to $X_1+(X_2-X_1)/2$, and one applies the same rule for points on the vertical axis, a small octagon can be defined by connecting these four new points on the axes and the same four corners of the rectangle (Fig. 2), denoted the "Small Octagonal Shape".

In the ACI seismic design provisions (ACI, 1999), the requirements for transverse reinforcements are prescribed as:

$$A_{sh} \geq 0.3\left(\frac{sh_c f_c'}{f_{yh}}\right)\left(\frac{A_g}{A_{ch}} - 1\right) \tag{8}$$

$$A_{sh} \geq 0.09 sh_c \frac{f_c'}{f_{yh}} \tag{9}$$

where A_{sh} is the total transverse steel cross-sectional area within spacing s; h_c is the cross-sections of the column core measured from center-to-center of the confining reinforcement; A_g is the gross area of the column section; A_{ch} is the cross sectional area of a column measured out-to-out of the transverse reinforcements; f_c' is the specified compressive strength of the concrete; f_{yh} is the specified yield strength of the transverse reinforcement. From Eqs. (8) and (9), the equivalent transverse pressure of the concrete can be defined as:

$$\frac{A_{sh} f_{yh}}{sh_c} \geq 0.3 f_c'\left(\frac{A_g}{A_{ch}} - 1\right) \tag{10}$$

$$\frac{A_{sh} f_{yh}}{sh_c} \geq 0.09 f_c' \tag{11}$$

If the amount of transverse reinforcement in the existing columns is not enough to satisfy the requirements prescribed in Eqs. (10) and (11), then the additional confining pressure must be provided by external jacketing. The relationship between the additional lateral confinement and the tensile stress in the jacket can be evaluated using the static equilibrium. As shown in Fig. 3, the free body diagram can be cut either from the centerline of the column section (Type I) or near the corners (Type II). The octagonal jacket is to prevent the outward bulging tendency of the rectangular section by mobilizing the tensile strength of the jacketing material. For a rectangular cross section oriented as shown in Fig. 2, it is found by examining typical values of $\sin\theta$ and $\cos\alpha$ in Fig. 3, that, for the same demand of lateral confinement, the tensile stress in the jacket near the column corner (Type II) is much higher than that near the centerline of the section (Type I). Therefore, the Type II free body cut near the edge of the section is used in this research. Thus, the requirements for transverse pressure on the concrete can be expressed as:

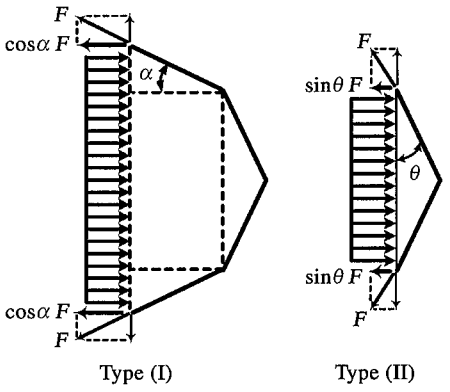

Fig. 3 Lateral confinement of octagonal jacket

$$\frac{2F\sin\theta}{B} + \frac{A_{sh} f_{yh}}{sh_c} \geq \{0.3 f_c'\left(\frac{A_g}{A_{ch}} - 1\right), 0.09 f_c'\}_{\max} \tag{12}$$

where B is the cross-section width of the column. In Fig. 3, the tensile strength provided by the octagonal steel jacketing for a unit length of the column is:

$$F = t_{sj} f_{ysj} \tag{13}$$

where t_{sj} is the thickness of the steel jacket; f_{ysj} is the specified yield strength of the steel jacket. Thus, the required thickness of the octagonal steel jacket can be calculated as:

$$t_{sj} = \frac{B}{2\sin\theta f_{ysj}}\{\{0.3 f_c'\left(\frac{A_g}{A_{ch}} - 1\right), 0.09 f_c'\}_{\max} - \frac{A_{sh} f_{yh}}{sh_c}\} \tag{14}$$

For CFRP material, the tension strength for a unit length of the column can be expressed as:

$$F = t_{frp} f_{ufrp} \tag{15}$$

where t_{frp} is the total thickness of the CFRP sheets; f_{ufrp} is the ultimate strength of the CFRP sheet. Thus, the required thickness of the CFRP sheets is:

$$t_{frp} = \frac{B}{2\sin\theta f_{ufrp}}\{\{0.3 f_c'\left(\frac{A_g}{A_{ch}} - 1\right), 0.09 f_c'\}_{\max} - \frac{A_{sh} f_{yh}}{sh_c}\} \tag{16}$$

Table 1 Summary of material strength

Unit: MPa	Concrete Strength	#5 Longitudinal Reinforcement	ϕ6 Transverse Reinforcement	4.5 mm Steel Jacket (f_{ysj})	2.3 mm Steel Jacket (f_{ysj})	Infilled Cement
Design	21	280	420	252	252	42
Measured	25	363	609	294	350	59

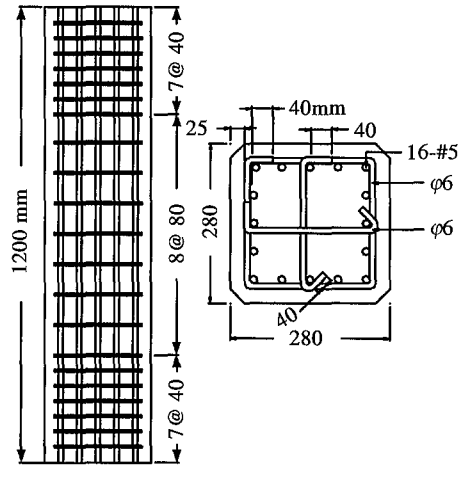

Fig. 4 Details of test specimens

Table 2 CFRP (MRL-T7-250) properties

Ultimate Strength f_{ufrp}	3550 MPa
Elastic Modulus E_j	2.35×10^5 MPa
Thickness per layer	0.1375 mm
Ultimate strain	0.015
Unit weight	250 g/m^2

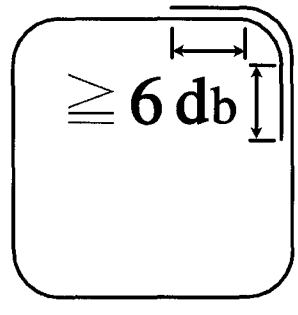

Fig. 5 Typical transverse reinforcement details adopted before 1999 Chi-Chi Taiwan Earthquake

III. EXPERIMENTAL PROGRAM

1. Test Matrix

A total of 12 specimens were constructed and tested under monotonically applied axial compression. One of the specimens is the benchmark, 7 specimens were retrofitted using steel jacketing, and 4 specimens using CFRP jacketing. The reinforcing details of the specimens are shown in Fig. 4. The height of the specimens is 1200mm, and the cross section is 280mm by 280mm. The longitudinal reinforcements of the column specimens consist of 16-#5 (16mm diameter), uniformly distributed along the four sides of the column cross-section. The transverse reinforcements of the specimens are ϕ6 (6mm diameter), spaced at 40mm on center in the middle potential plastic hinge zone, and spaced at 80mm outside that region (Fig. 4). Fig. 5 shows typical transverse reinforcement details commonly adopted in Taiwan. The 90 degree, not 135 degree, non-ductile hook detail is believed one of the key factors responsible for many column failures observed after the 1999 Chi-Chi Taiwan Earthquake. Accordingly, this type of transverse reinforcement arrangements is adopted for all specimens. All of the specimens were constructed using the same reinforcing materials and concrete batches. The nominal and the measured strength of the materials are shown in Table 1. The CFRP sheets were provided by the Materials Research Laboratory of the Industrial Technology Research Institute. The material properties of the CFRP sheets are listed in Table 2. Non-shrink cement was used as infilling material between the square columns and the jackets.

2. Steel Jacketed Specimens

The dimensions of the steel jacketed specimens are shown in Fig. 6. The steel jacket tubing was prefabricated in the shop before deliver to the laboratory at the NCREE. The shapes of the steel jacketing include circular, rectangular, large octagonal and, small or reduced octagonal. The thicknesses of the octagonal steel jackets were calculated based on the design criteria noted in Eq. (14). Specimens LOS23A and LOS23B were retrofitted using the large octagonal shape and the thickness of the steel jacket was 2.3mm. Specimens ROS45A and ROS45B were retrofitted using the reduced octagonal shape and the thickness of the steel jacket was 4.5mm. Specimen CS23 was retrofitted by a circular jacket, and the thickness

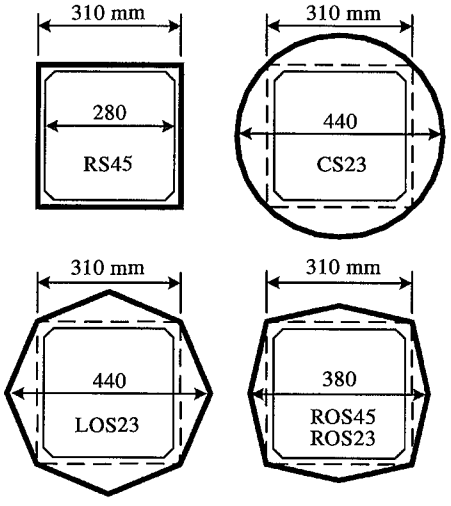

Fig. 6 Steel jacketing schemes

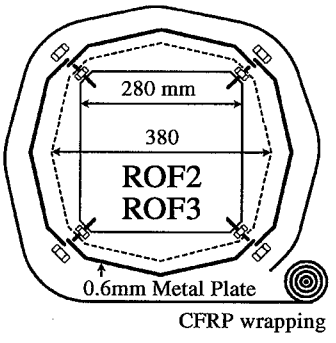

Fig. 7 Octagonal CFRP jacketing procedure

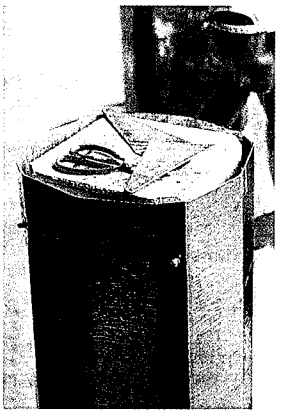

Fig. 8 CFRP wrapping

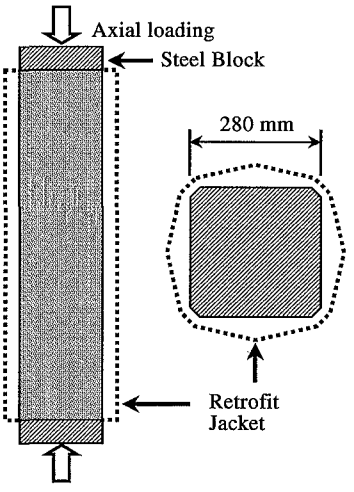

Fig. 9 Concentric loading test

of the jacket was a 2.3mm, the same as Specimen LOS23A. Specimen RS45 was retrofitted by a 4.5mm rectangular jacket; the thickness is the same as in Specimen ROS45A for the purpose of comparison. Specimen ROS23 is a reduced octagonal jacketed specimen using a 2.3mm thick jacket, just half the thickness of that in Specimen ROS45A, in order to see whether the design criteria noted above are conservative enough or not.

3. CFRP Jacketed Specimens

The shapes of the CFRP jackets include rectangular and reduced octagonal. In order to provide lateral confinement, continuous CFRP sheets were wrapped in the transverse direction of the columns. Specimen ROF2 and ROF3 were retrofitted, using the reduced octagonal scheme with 2 and 3 layers, respectively, of CFRP wrapping. The layers of CFRP were calculated by conservatively applying the design criteria noted in Eq. (16). It is worth noting that the assembling procedures for the reduced octagonal CFRP wrapping specimens are novel, as shown in Fig. 7. The octagonal shape was first formed using four 0.6mm thick galvanized metal sheets that were bent into the specified shape before being attached to each other by screws. Then, CFRP wrapping was done after the metal surface was smoothed, as shown in Fig. 8. The final procedure was infilling with non-shrink cement. The CFRP wrappings for Specimens RF2 and RF3 were 2 and 3 layers, respectively. They were rectangular, and the number of layers was the same as those in the reduced octagonal specimens for comparison purposes. The corner radius R is 30mm according to the standard CFRP wrapping procedures.

4. Testing Method

As shown in Fig. 9, all specimens were loaded under monotonically increasing concentric compressive strains. At each end of the specimen, a steel square loading block was positioned in order to ensure that the axial load was applied only to the rectangular RC column section. As shown in Figs. 10

Table 3 Specimen details and test results

Specimen	Jacket Thickness (mm)	*Pmax* (kN)	*Pmax/Pn*	ε_{Pmax} (%)	ε_{stop} (%)	Note
BM	NA	2960	1.03	0.41	1.43	Benchmark
RS45	4.5	4270	1.49	1.6	5.16	Rectangular Steel Jacketing
CS23	2.3	7340	2.56	4.73	4.99	Circular Steel Jacketing
LOS23A	2.3	6725	2.35	3.73	5.37	Large Octagonal Steel Jacketing
LOS23B		6485	2.27	4.84	5.30	
ROS45A	4.5	6310	2.20	3.82	5.27	Reduced Octagonal Steel Jacketing
ROS45B		6450	2.25	4.29	5.25	
ROS23	2.3	5710	2.00	3.61	5.12	Reduced Octagonal Steel Jacketing
Specimen	CFRP Layers	*Pmax* (kN)	*Pmax/Pn*	ε_{Pmax} (%)	ε_{stop} (%)	Note
RF2	2	3810	1.33	1.33	1.66	Rectangular CFRP wrapping
RF3	3	4425	1.56	2.57	2.90	
ROF2	2	6020	2.10	2.54	2.57	Reduced Octagonal CFRP wrapping
ROF3	3	6170	2.16	2.52	2.55	

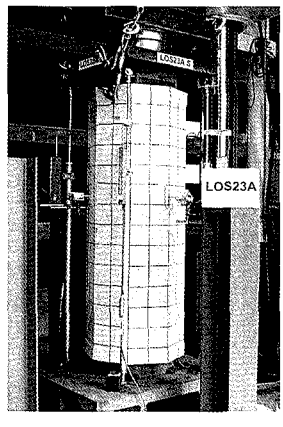

Fig. 10 Test setup (NTU)

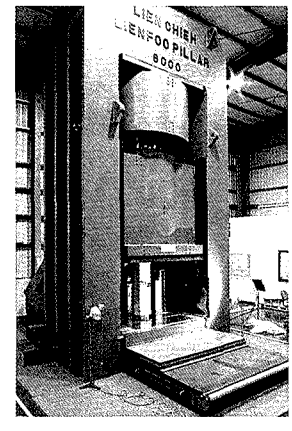

Fig. 11 Test setup (Lien-Foo)

and 11, the tests were conducted using the NTU's Shimadzu 4900kN and Lien-Foo 58800kN universal testing machines with a 2.5×10^{-5} (0.03mm/sec) strain rate. Tests stopped when severe damage occurred or the axial strain exceeded 5%.

The THS-1100 data logger and SHW-50*D* switch box made by TML were employed for data collection during the tests. External LVDTs were used for measuring the longitudinal and lateral deformations of the specimens. Strain gages were also aligned on the reinforcements and the jacket surfaces in each specimen for further data analysis.

IV. EXPERIMENTAL RESULTS

Experimental results of axial loading tests are summarized in Table 3. The ratio between the peak axial strength and the nominal axial capacity (*Pmax/Pn*) of each specimen is also given in the table. The nominal axial capacity is computed from $Pn=0.85f_c' A_g+F_yA_s$, where f_c' and F_y are the measured yielding stress of reinforcing steel. The axial load versus strain response relationships for the steel and CFRP jacketed specimens are shown in Figs. 12 and 13, respectively. The comparisons for the steel and CFRP jacketing are shown in Fig. 14. The failure modes of the specimens after the tests are shown in Figs. 15 and 16.

1. Response of the Benchmark Specimen

The response of the benchmark specimen *BM* is

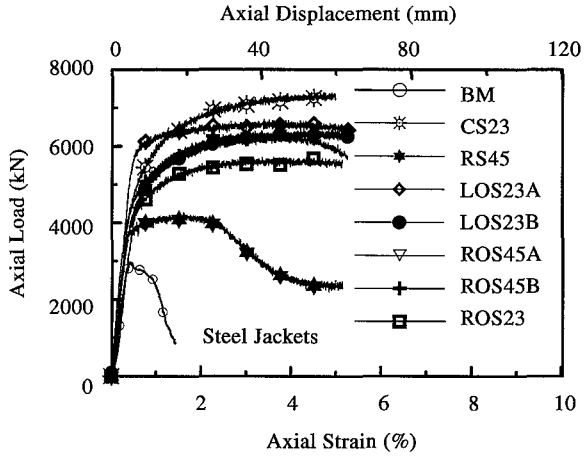

Fig. 12 Axial force versus strain relationships of steel jacketed specimens

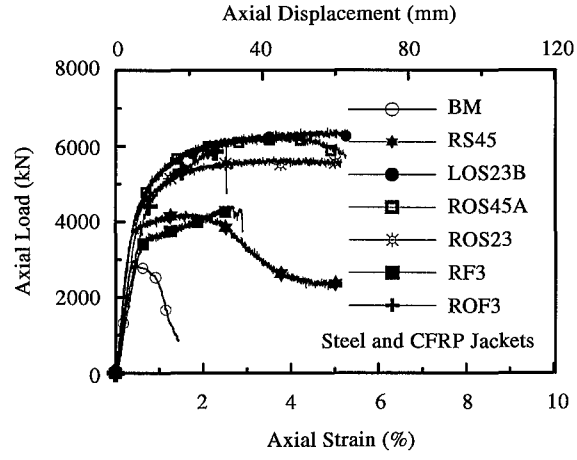

Fig. 14 Axial force versus strain relationships for steel and CFRP jacketed specimens

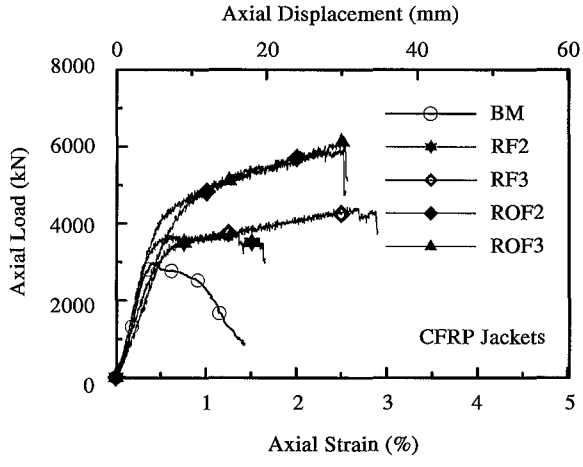

Fig. 13 Axial force versus strain relationships of CFRP jacketed specimens

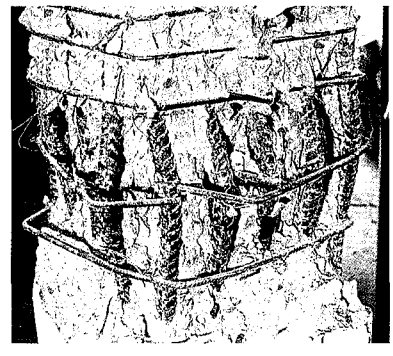

Fig. 15 Spec. BM after testing

shown in Fig. 12. The peak load is 2960kN, which is very close (1.03:1) to the nominal strength 2862kN. In the axial load versus strain response curve, it is evident that the strength degraded rapidly after the peak load was reached. Fig. 15 shows evidence of open-up of the transverse reinforcements when loose concrete was removed after the test. This failure mode is very similar to that observed in the actual building damage shown in Fig. 1. The non-ductile behavior of this type of transverse reinforcing details has been confirmed in the column axial load versus strain response curve.

2. Response of the Steel Jacketed Specimens

The response curves of the steel jacketed specimens are shown in Fig. 12. Tests were stopped at about 5% axial strain for all specimens. Except for the rectangular steel jacketed Specimen RS45, all other circular or octagonal steel jacketed specimens exhibited excellent axial strength and axial ductility performance. Even at the peak 5% axial strain, their axial strengths sustained very well. Specimen RS45 was retrofitted using a 4.5mm-thick rectangular steel jacket. Due to premature outward bulging at a small column axial strain, its improvements on column axial strength and axial ductility are much less pronounced than those of other steel jacketed specimens. Specimen CS23 had the highest axial strength, suggesting that the circular retrofit scheme has excellent performance in axial strength and axial ductility. It should be noted that Specimen LOS23A was tested again using the Lien-Foo 58800kN machine due to the limited loading capacity of NTU's Shimadzu 4900kN machine. Specimen LOS23A has higher strength performance than that of the same design Specimen LOS23B, possibly due to the recompression situation. Specimens LOS23B, ROS45A and ROS45B all have very similar axial load versus strain response curves, suggesting the assumptions and calculations made for

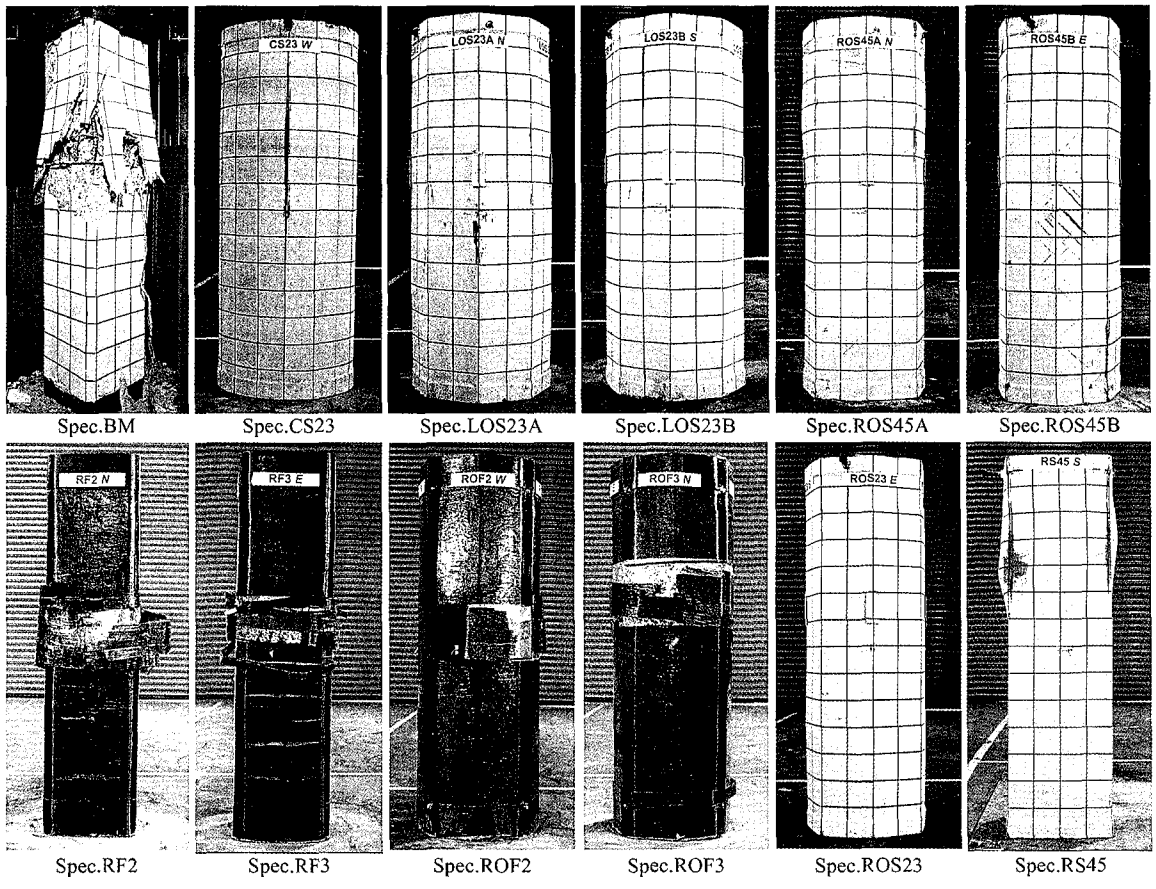

Fig. 16 Final appearance of specimens

the lateral confinement are reasonable. The peak axial strength of Specimen ROS23 is less than that of ROS45A, but Specimen ROS23 still exhibited excellent axial ductility performance, suggesting that the design criteria noted above is on the conservative side. The strength ratio *Pmax/Pn* for circular jacketed specimen CS23 is 2.56, for rectangular steel jacketed specimen RS45 it is 1.49, and for other octagonal steel jacketed specimens it is equal to or greater than 2.0.

3. Response of the CFRP Jacketed Specimens

The axial load versus strain response curves of the CFRP wrapped specimens are shown in Fig. 13. The general effects of the CFRP material can be observed as the column axial strength continued to rise until the CFRP ruptured as shown in Fig. 13. The final damage and ruptured positions of CFRP wrapped specimens are shown in Fig. 16. The CFRP sheets ruptured in the middle of Specimen RF2 at an axial strain of 1.5%, the other three CFRP jacketed specimens started to rupture at a strain of about 2.5%. It is evident that the wrapping and the curing must be done very carefully or the CFRP may fracture prematurely. The outward bulging phenomenon observed in Specimen RF2 and RF3 was not as pronounced as that which occurred in RS45. It appears that well smoothed corners prepared for CFRP wrapping process have made each corner a good place to develop confinement and reduced the unconfined length of the core concrete of the scaled down specimens. Tests also confirm that the octagonal scheme is more efficient than the rectangular scheme in developing the axial strength and axial ductility performance of CFRP jacketed columns. It is noted, in Fig. 13, that the CFRP jacketed Specimens ROF2 and ROF3 wrapped with either 2 or 3 layers CFRP sheets have very similar axial force versus deformation responses. This observation concurs with the findings in other tests (Li *et al.*, 2000), suggesting that the overall confining effects of the CFRF sheets are limited. If the confining limit is reached, the marginal effects of the additional layer are almost negligible.

The strength ratios *Pmax/Pn* for rectangular CFRP jacketed specimens RF2 and RF3 are 1.33 and 1.56, respectively. These values are very close to the results of the rectangular steel jacketed specimen RS45 (*Pmax/Pn*=1.49). For the octagonal CFRP jacketed specimens ROF2 and ROF3, their strength ratios are greater than 2.0.

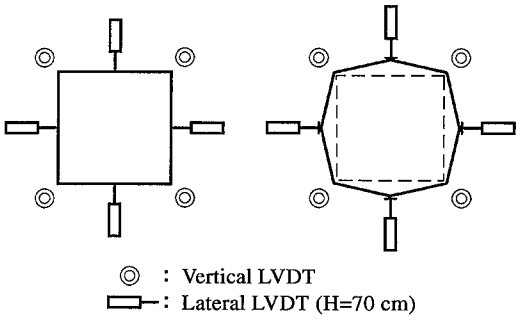

Fig. 17 External measuring arrangement

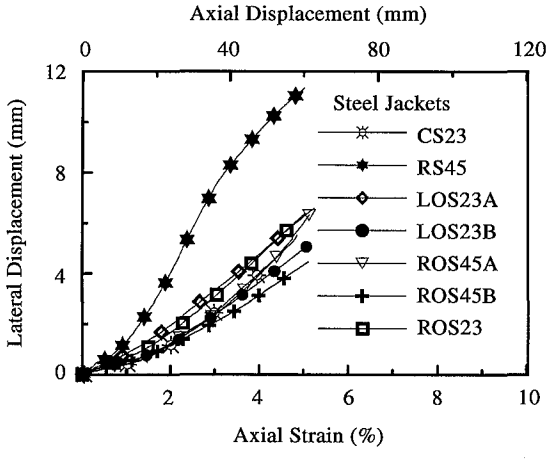

Fig. 18 Lateral deformations of steel jacketed specimens

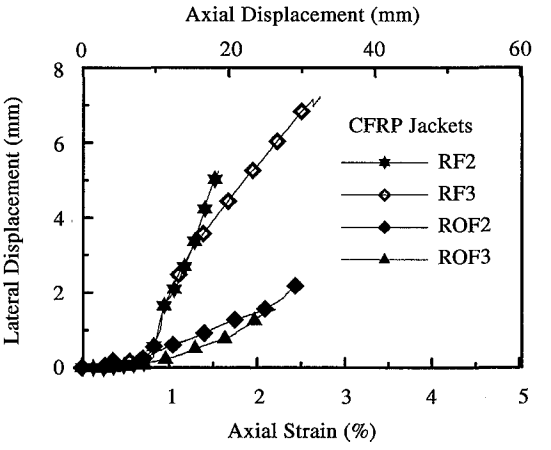

Fig. 19 Lateral deformations of CFRP jacketed specimens

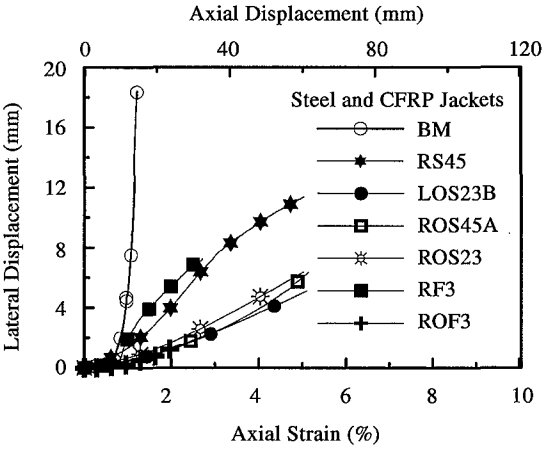

Fig. 20 Lateral deformations for steel and CFRP jacketed specimens

V. DISCUSSION OF TEST RESULTS

In order to monitor the column lateral outward deformations, LVDTs were arranged on the two axes, 70cm-high on the specimen, as shown in Fig. 17. Figs. 18, 19 and 20 show the average lateral deformation response curves of all specimens. In Figs. 18 and 19, it can be seen that the lateral deformations of the rectangular jacketed specimens are larger than the circular or octagonal jacketed specimens. Steel or CFRP rectangular jackets have similar trends of lateral deformation. The lateral bulge out deformation is the primary reason why rectangular jacketed specimens have a lower axial strength than the circular or octagonal jacketed specimens. It is evident that the rectangular jacket is not effective in providing lateral confinement.

It can be seen from the material strengths listed in Tables 1 and 2 that the strength of 2 layers of CFRP sheets, used in the tests, is equivalent to a 2.8 mm thick layer of steel having 350MPa yield strength. Similarly, the strength of 3 layers CFRP sheets is about the same as a 4.9mm thick steel plate considering the yield strength of 294MPa. Therefore, strictly speaking, results of steel jacketed specimens using the 2.3mm (f_{ysj}=350MPa) or the 4.5mm (f_{ysj}=294MPa) thick steel plate might not be suitable for direct comparison with the results of 2 or 3 layer CFRP jacketed tests. Nevertheless, judging the small differences in the corresponding designs (2.3mm versus 2.8mm or 4.5mm versus 4.9mm), test results of these steel jacketed specimens should provide a conservative basis for evaluating the effectiveness of the steel jackets in enhancing the column axial load carrying performance. From the axial load versus axial strain responses of steel and CFRP jacketed specimens given in Fig. 14, it is confirmed that both steel jacketed and CFRP jacketed specimens have very similar trends in developing the axial load carry capacity. The peak axial strength developed in Specimens ROS23 (steel jacketed) and ROF3 (CFRP wrapped) is very similar. It is evident that the steel jacket provides primarily lateral confinement as the fibers in the CFRP sheets are oriented in the transverse direction. The axial strength effects of the steel jacket on the column axial

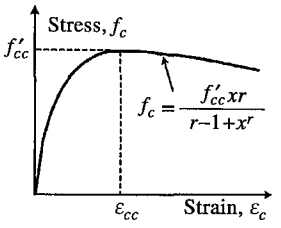

Fig. 21 Stress-strain model for confined concrete (Mander *et al.* 1988)

strength should be negligible.

For typical RC columns constructed with stirrups, the peak load is generally reached before 1% axial strain due to the buckling of the longitudinal reinforcements (Sheikh *et al.*, 1980; Mander *et al.*, 1988; Hoshikuma *et al.*, 1997). In this study, the axial strain at the peak load for the circular or octagonal jacketed specimens is greater than 2%. The buckling of the longitudinal reinforcements was essentially eliminated using the circular or octagonal jackets with continuous confining effects. Rapid degradation of strength could occur in the typical RC columns after peak strength is reached. However, test results confirm that octagonal steel jacketed specimens can maintain the axial load carrying capacity even under extremely large axial strain conditions.

Comparing the performance of steel and CFRP jacketed specimens, it is evident from Fig. 14 that the steel jacketing scheme can provide greater axial ductility than that of the CFRP jacket. The steel jackets were able to provide a stable lateral confinement even when a 5% axial strain was reached, but the CFRP jackets had already ruptured before 3% axial strain was reached.

VI. ANALYTICAL MODELS

In order to analyze the effects of steel jacketing in providing lateral confinement for concrete, the stress versus strain relationship (Fig. 21) for confined concrete suggested by Mander *et al.* (1988) is incorporated into an analytical column model. In this model, the longitudinal compressive concrete stress f_c is given by:

$$f_c = \frac{f'_{cc}xr}{r-1+x^r} \tag{17}$$

where f'_{cc} is the compressive strength of confined concrete.

$$f'_{cc} = f'_{co}\left(2.254\sqrt{1+\frac{7.94f'_l}{f'_{co}}} - \frac{2f'_l}{f'_{co}} - 1.254\right) \tag{18}$$

$$x = \frac{\varepsilon_c}{\varepsilon_{cc}} \tag{19}$$

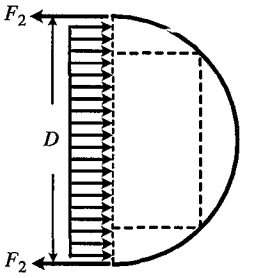

Fig. 22 Lateral confinement of circular jacket

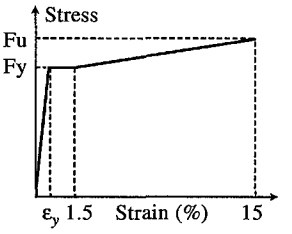

Fig. 23 Stress-strain model for longitudinal reinforcement

ε_c is the longitudinal compressive concrete strain.

$$\varepsilon_{cc} = \varepsilon_{co}\left[1 + 5\left(\frac{f'_{cc}}{f'_{co}} - 1\right)\right] \tag{20}$$

f'_{co} and ε_{co} are the unconfined concrete strength and corresponding strain, respectively.

$$r = \frac{E_c}{E_c - E_{\sec}} \tag{21}$$

where E_c is the tangent modulus of elasticity of the concrete.

$$E_c = 5000\sqrt{f'_{co}}\,MPa \tag{22}$$

$$E_{\sec} = \frac{f'_{cc}}{\varepsilon_{cc}} \tag{23}$$

For the octagonal jacket, the effective lateral confining stress f'_l is computed as follows:

$$f'_l = \frac{2F\sin\theta}{B} + \frac{A_{sh}f_{yh}}{sh_c} \tag{24}$$

For the circular jacket, the effective lateral confining stress f'_l is computed as follows considering the static equilibrium diagram given in Fig. 22:

$$f'_l = \frac{2F}{D} + \frac{A_{sh}f_{yh}}{sh_c} \tag{25}$$

In this axially loaded column model, a tri-linear stress versus strain relationship as shown in Fig. 23 is considered for the reinforcing steel. The F_y and F_u

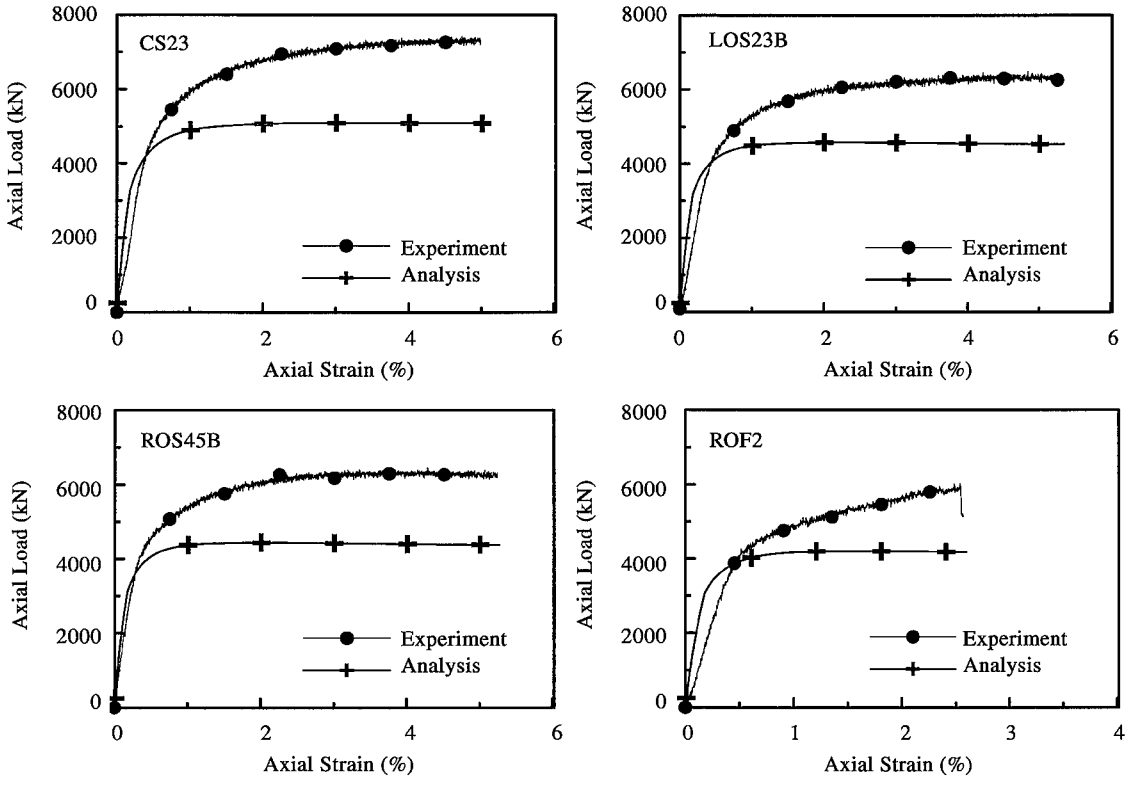

Fig. 24 Analytical and experiment axial force versus strain relationships for Specimens

are the measured yield and ultimate strength of the longitudinal reinforcement. The yield strain ε_y is calculated from F_y/E_s, where E_s=200,000MPa. 1.5% strain, for the end of the perfectly plastic flow, is adopted and the strain corresponding to ultimate strength is set at 15%.

Assuming plane remains plane under the axial load, the analytical axial force versus strain relationships are compared with the experimental results in Fig. 24 for three octagonal and one circular jacketed specimen. The lateral concrete confinement for the octagonal steel or CFRP jacketed specimens is computed from the static equilibrium based on the Type II free body diagram given in Fig. 3. The analytical axial strength is significantly less than the experimental results as shown in Fig. 24. This confirms that the axial strength of the octagonal jacketed specimens can be predicted rather conservatively if the analytical models noted above are applied. Nevertheless, based on the observations made during the tests, a somewhat deformed shape for jackets under the high axial strain can be assumed for further analysis (Tsai and Lin, 2002). It has been found that a much better simulation of the experimental responses of the octagonal jacketed specimens can be achieved by increasing the steel jacket membrane force angle θ defined in Fig. 3. However, when the peak loads were developed the real deformed angles of the octagonal jackets were not measured during the tests. Thus, except for trial and error, it is not possible to solve for possible orientations of the deformed octagonal jackets. In addition, the stress in the steel jackets is likely higher than the yield stress adopted in computing the confinement. This is evidenced by the column axial strain versus hoop strain relationships given in Fig. 25. Under large axial load, the steel jackets have passed the yield point and gone well into the strain hardening range. Although a 280×280mm square steel block has been placed at each end of the column specimen during the tests, as noted before, test results indicate that peak load developed in the steel jacketed specimens somehow depends on the gross area of the retrofitted specimens. For example, the order of the *Pmax/Pn* ratios is CS23>LOS23>ROS23. This finding seems to suggest that the infill material between the square cross section and the external jacketing could have participated in resisting the column axial load effects. It also helps to explain why the analytical models fail to satisfactorily predict the experimental responses if the axial load carrying participations of the material outside the square cross section are completely neglected. Finally, Mander's confined concrete model, developed for axially loaded members constructed with

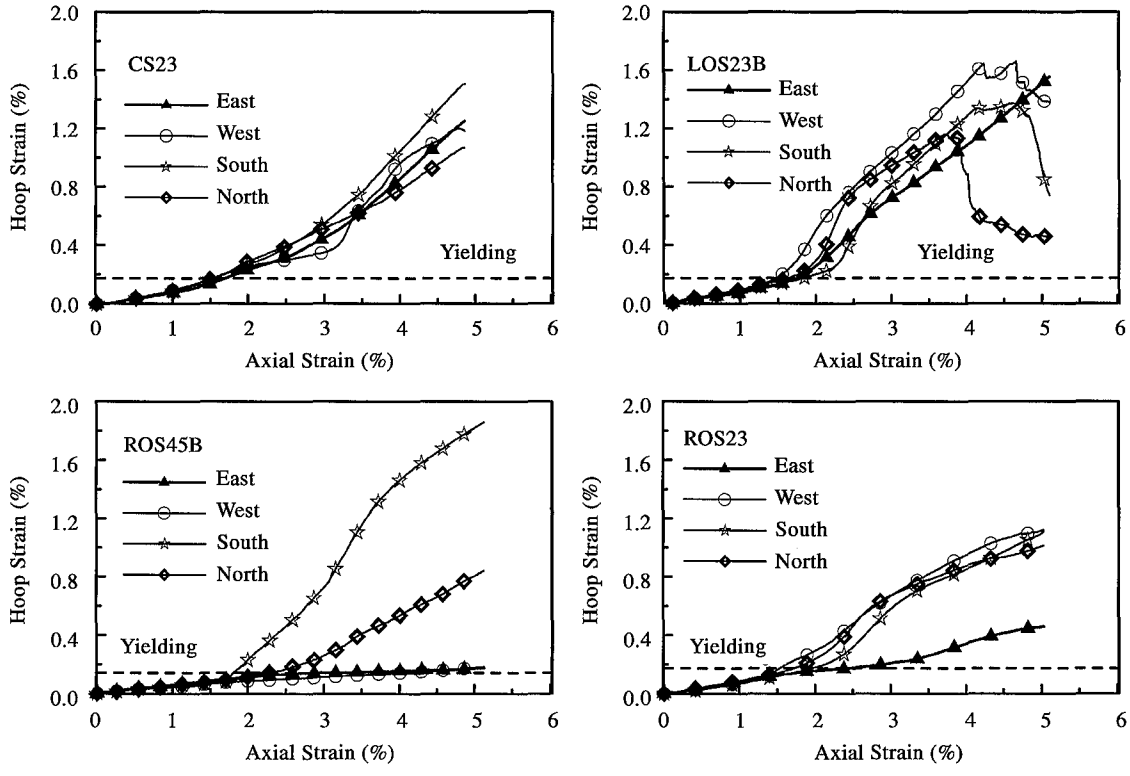

Fig. 25 Confinement strain of steel jacketing specimens

transverse ties, might not be perfectly applicable for specimens using external continuous jackets (Li *et al.*, 2000).

VII. CONCLUSIONS

Based on the experimental and analytical results, the following conclusions can be drawn.

1. Rectangular RC columns using 90 degree transverse reinforcement hook details are not able to provide adequate confinement to sustain high axial compressive load demands, and non-ductile brittle failure may rapidly occur after reaching the peak strength.
2. The proposed octagonal jacketing scheme can effectively provide lateral confinement thereby enhancing strength and ductile performance under high axial strain demands.
3. The outward bulging phenomenon of the rectangular jacket is evident. Rectangular jackets are not effective in providing lateral confinement for concrete.
4. The octagonal CFRP jacket can provide lateral confinement more effectively than the rectangular CFRP jacket.
5. The proposed octagonal jacketing design methodology can be applied effectively and conservatively to improve the performance of RC columns subjected to high axial loads.
6. Tests confirm that the steel and the CFRP octagonal jackets can improve the column axial strength to more than 2 times of nominal strength. For the same thickness of steel plate or CFRP wrap, the effects are much less pronounced when the jackets are square-shaped.
7. Analytical results suggest that the effects of steel jacketing in enhancing the column axial force versus deformation relationships can be very conservatively predicted by incorporating the tri-linear model for reinforcing steel and Mander's confined concrete model.
8. Experimental and analytical results suggest that the proposed octagonal steel jacketing scheme is suitable for seismic retrofit of existing RC concrete columns deficient in meeting high axial load demands.
9. This paper investigates the effectiveness of various external jacketing techniques commonly found or potentially useful at the construction site. Based on the test and analytical results, the strength and ductility capacities of the rectangular RC column using the proposed octagonal jacketing scheme can be conservatively estimated. Recent tests have confirmed the effectiveness of the reduced octagonal steel jacketing in large bridge pier retrofit. However, further research on large building

columns is needed to warrant their application in seismic retrofit of RC columns with high axial load risks.

ACKNOWLEDGMENTS

The financial support provided by the National Science Council and the National Center for Research on Earthquake Engineering is gratefully acknowledged. The experimental facilities and the technical support provided by the NTU Joint Laboratory for Solid Mechanics and Lien-Foo Pillar Rubber Bearing Co. are very much appreciated.

NOMENCLATURE

A_{ch}	the cross sectional area of a column measured out-to-out of the transverse
A_g	the gross area of the column section
A_{sh}	the total transverse steel cross-sectional area
B	the cross-section width of the column
E_c	the tangent modulus of elasticity of the concrete
f_c'	the specified compressive strength of the concrete
f_c	the longitudinal compressive concrete stress
f_{cc}'	the compressive strength of confined concrete
f_{co}'	the unconfined concrete strength and corresponding strain
f_l'	the effective lateral confining stress
f_{yh}	the specified yield strength of the transverse reinforcement
f_{ysj}	the specified yield strength of the steel jacket
f_{ufrp}	the ultimate strength of the CFRP sheet
F_y	the yield strength of the longitudinal reinforcement
F_u	the ultimate strength of the longitudinal reinforcement
h_c	the cross-section dimension of the column core measured from center-to-center of the confining reinforcement
s	the spacing of the transverse steel
t_{frp}	the total thickness of the CFRP sheets
t_{sj}	the thickness of the steel jacket
X_2, Y_2	the long and short axes of the ellipse
ε_c	the longitudinal compressive concrete strain
ε_{co}	the unconfined concrete strength and corresponding strain

REFERENCES

1. ACI Committee 318, 1999, *Building Code Requirements for Structural Concrete and Commentary*, ACI 318-99, American Concrete Institute, Farmington Hills.
2. Harries, K. A., Ricles, J. M., Sause, R., Pessiki, S., and Walkup, S. L., 1999, "Seismic Retrofit of Non-ductile Reinforced Concrete Building Columns using FRPC Jackets," *Proceedings of the Sixth U.S. National Conference on Earthquake Engineering*, Seattle, Washington, U.S.
3. Hoshikuma, J., Kawashima, K., Nagaya, K., and Taylor, A.W., 1997, "Stress-Strain Model for Confined Reinforced Concrete in Bridge Piers," *Journal of Structural Engineering*, ASCE, Vol. 123, No. 5, pp. 624-633.
4. Li, Y. F., Hwang, J. S., Chu, Y. C., Hsieh, Y. M., Song, Y. I., and Kuo, M. I., 2000, "A Study on the Circular Section Bridge Column Retrofitted by Using Steel and CFRP Jacketing," *Proceedings of the Second International Workshop on Mitigation of Seismic Effects on Transportation Structures*, Taipei, Taiwan, pp. 23-42.
5. Mander, J. B., Priestley, M. J. N., and Park, P., 1988, "Observed Stress-Strain Behavior of Confined Concrete," *Journal of Structural Engineering, ASCE*, Vol. 114, No. 8, pp. 1827-1849.
6. Mander, J. B., Priestley, M. J. N., and Park, P., 1988, "Theoretical Stress-Strain Model for Confined Concrete," *Journal of Structural Engineering, ASCE*, Vol. 114, No.8, pp. 1804-1826.
7. Sheikh, S. A., and Uzumeri, S. M., 1980, "Strength and Ductility of Tied Concrete Columns," *Journal of the Structural Division, ASCE*, Vol. 106, No. 5, pp. 1079-1102.
8. Sun, Z. L., Seible, F., and Priestley, M. J. N., 1993, "Flexural Retrofit of Rectangular Reinforced Concrete Bridge Columns by Steel Jacketing," Structural System Research Project Report, No. SSRP-93/01, Department of Applied Mechanics and Engineering Science, U.C. San Diego.
9. Tsai, K. C., and Lin, M. L., 2002, "Experimental Axial Load Carrying Performance of Rectangular RC Building Columns Retrofitted by Steel or CFRP Jacketing," Technical Report, National Center for Research on Earthquake Engineering.
10. Tsai, K. C., and Lin, M. L., 2001, "Steel Jacket Retrofitting of Rectangular RC Bridge Columns to Prevent Lap-spliced and Shear Failure," Technical Report, National Center for Research on Earthquake Engineering.
11. Tsai, K. C., Chang K. C., Lin M. L., and Chung, F. S., 2000, "Seismic Retrofit of Rectangular RC Bridge Columns Using Steel and FRP Jackets," *Proceedings of the Second International Workshop on Mitigation of Seismic Effects on Transportation Structures*, Taipei, Taiwan, pp. 90-105.

Manuscript Received: Aug. 22, 2001
Revision Received: Mar. 12, 2002
and Accepted: Apr. 09, 2002

鋼筋混凝土柱受高軸向力之行為與耐震補強研究

蔡克銓　林敏郎

國立台灣大學土木工程學研究所

摘　要

本研究根據集集地震前台灣工程上普遍採用之箍筋細節，製做方形鋼筋混凝土柱試體並進行軸向載重試驗，採用不同之包覆補強方式以探討其耐震補強效果。包覆形狀包括圓形、方形與八邊形，而補強材料採用鋼板及碳纖維複合材料。由單向軸壓試驗結果顯示，未補強標準試體的破壞模式與集集地震中許多鋼筋混凝土柱破壞案例類似。標準試體之強度雖可發展至標稱設計強度，但在超過極限強度後即迅速產生無韌性破壞。實驗結果亦顯示，鋼板與碳纖之矩形包覆補強效果較不理想，但八邊形鋼板包覆補強試體於提升柱軸向強度與韌性上均有優良的表現。碳纖維複合材料可有效提升柱軸向強度，但於高軸向應變下會發生無預警地脆性斷裂破壞。碳纖維複合材料無法如鋼板般改善鋼筋混凝土柱之韌性性能，但所提出之八邊形碳纖維包覆方式較相同層數下之矩形碳纖維包覆試體有更佳之補強效果。所有採用八邊形包覆之鋼板或碳纖維補強試體，其軸向強度均可提升至柱標稱軸向強度的兩倍以上。

關鍵詞：鋼板包覆，碳纖維複合材料包覆，八邊形補強斷面。